Thrombin Hydrolysis of V29F and V34L Mutants of Factor XIII (28−41) Reveals Roles of the P_9 and P_4 Positions in Factor XIII Activation†

Toni A. Trumbo and Muriel C. Maurer*

Department of Chemistry, University of Louisville, Louisville, Kentucky 40292

Received September 19, 2001; Revised Manuscript Received November 15, 2001

ABSTRACT: In blood coagulation, thrombin helps to activate factor XIII by cleaving the activation peptide at the R37−G38 peptide bond. The more easily activated factor XIII V34L has been correlated with protection from myocardial infarction. V34L and V29F factor XIII mutant peptides were designed to further characterize substrate binding to thrombin. HPLC kinetic studies have been carried out on thrombin hydrolysis of FXIII activation peptide (28−41), FXIII (28−41) V34L, FXIII (28−41) V29F, and FXIII (28−41) V29F V34L. The V34L mutations lead to improvements in both K_m and k_{cat} whereas the V29F mutation primarily affects K_m. Interactions of the peptides with thrombin have been monitored by 1D proton line broadening NMR and 2D transferred NOESY studies. The results were compared with previously published X-ray crystal structures of thrombin-bound fibrinogen Aα (7−16), thrombin receptor PAR1 (38−60), and factor XIII (28−37). In solution, the ^{34}VVPR^{37} and ^{34}LVPR^{37} segments of the factor XIII activation peptide serve as the major anchor points onto thrombin. The N-terminal segments are proposed to interact transiently with the enzyme surface. Long-range NOEs from FXIII V29 or F29 toward ^{34}V/LVPR^{37} have not been observed by NMR studies. Overall, the kinetic and NMR results suggest that the factor XIII activation peptide binds to thrombin in a manner more similar to the thrombin receptor PAR1 than to fibrinogen Aα. The V29 and V34 positions affect, in different ways, the ability of thrombin to effectively hydrolyze the activation peptide. Mutations at these sites may prove useful in controlling factor XIII activation.

Thrombin, a serine protease, plays an integral role in the latter stages of the blood-clotting cascade. Fibrinogen circulates in the blood as $(A\alpha B\beta\gamma)_2$. Thrombin cleaves the Arg^{16}−Gly^{17} peptide bond of the fibrinogen Aα chain and the Arg^{14}−Gly^{15} peptide bond of the fibrinogen Bβ chain, thereby releasing fibrinopeptides A and B to give fibrin. Fibrin monomers associate noncovalently to form an insoluble loose polymer network or soft clot (reviewed in ref *1*). Thrombin also activates factor XIII by hydrolyzing the Arg^{37}−Gly^{38} peptide bond and releasing the activation peptide (FXIII AP).[1] Factor XIII catalyzes the formation of γ-glutamyl-ε-lysyl covalent cross-links involving fibrin α and γ chains and incorporates fibronectin and α_2-antiplasmin. The cross-linked fibrin network creates a thrombolytically resistant hard clot. The thrombin receptor PAR1 is activated by thrombin hydrolysis of the Arg^{41}−Ser^{42} bond. The new N-terminus becomes a tethered ligand for PAR1. Binding of this ligand is followed by internalization of the receptor and a signal cascade (*2*). Thrombin also participates in the thrombolytic cascade by activating protein C in the presence of thrombomodulin (*3*).

Thrombin, although versatile, is not as promiscuous as other serine proteases. Insertion loops on the surface of the enzyme limit substrate access to the active site cleft. The active site is buried deeply within the cleft and is flanked by substrate recognition sites (*4*). The substrate amino acid sequence on the N-terminal side of the scissile bond makes significant contributions to binding and hydrolysis rates. The optimal peptide substrate or inhibitor of thrombin (*5*, *6*) has F/VPR in the P_3−P_1 substrate sites.[2] Amino acids beyond these positions can also play important roles. Table 1 shows a series of peptide sequences based upon natural substrates of thrombin. Key structural features of the peptides are summarized below.

The X-ray crystal structure of a fibrinopeptide A segment, Fbg Aα (7−16), bound to thrombin demonstrates a unique binding mode (*10*). Fbg Aα (7−16) has Val^{15} in place of the Pro at the P_2 position. The segment is engaged in a type

† This work was supported by a University of Louisville Competitive Enhancement Grant and an American Heart Association Grant-in-Aid Award (Ohio Valley Affiliate).

* To whom correspondence should be addressed. Tel: (502) 852-7008. Fax: (502) 852−8149. E-mail: muriel.maurer@louisville.edu.

[1] Abbreviations: FXIII, blood clotting factor XIII; AP, activation peptide; PAR1, protease activated receptor 1; Fbg Aα, peptide segment from the fibrinogen Aα chain; PEP1, FXIII AP (28−37) peptide 1 bound to thrombin (MOL1) in the asymmetric unit; PEP2, FXIII AP (28−37) peptide 2 bound to thrombin (MOL2) in the asymmetric unit; NMR, nuclear magnetic resonance; 1D, one dimensional; 2D, two dimensional; D_2O, deuterium oxide; DSS, sodium 2,2-dimethyl-2-silapentane-5-sulfonate; RP-HPLC, reverse-phase high-performance liquid chromatography; MALDI-TOF, matrix-assisted laser desorption ionization time of flight; K_m, Michaelis−Menten kinetic constant; k_{cat}, catalytic constant or turnover number; TOCSY, total correlation spectroscopy; NOESY, nuclear Overhauser effect spectroscopy.

[2] The P nomenclature system (..., P_3, P_2, P_1, P_1', P_2', P_3') is used to assign the individual amino acids positions on the substrate peptides (*7*). The P_1−P_1' peptide bond becomes hydrolyzed by the enzyme. The peptide amino acids to the left of the cleavage site are labeled P_2, P_3, P_4, etc. whereas those to the right of the cleavage site are labeled P_2', P_3', P_4', etc.

10.1021/bi0157823 CCC: $22.00
Published on Web 01/31/2002

Table 1: Amino Acid Sequences of Substrates and Inhibitors of Thrombin[a]

Factor XIII activation peptide segment	^{28}T**V**ELQG**V**V**PR**GVNL^{41}
Factor XIII activation peptide V34L segment	^{28}T**V**ELQG**L**V**PR**GVNL^{41}
Factor XIII activation peptide V29F segment	^{28}T**F**ELQG**V**V**PR**GVNL^{41}
Factor XIII activation peptide V29F V34L segment	^{28}T**F**ELQG**L**V**PR**GVNL^{41}
Fibrinogen Aα chain	^{7}D**F**LAEGGG**VR**GPRV^{20}
Thrombin Receptor PAR1 segment	^{32}KATNAT**L**D**PR**SFLL^{45}

[a] These human sequences were taken from the following sources: factor XIII (*8*), fibrinogen Aα chain (*9*), and thrombin receptor PAR1 (*2*).

I β-turn that returns Phe^8 to the active site, where it associates with Val^{15} in the aryl binding portion of the thrombin apolar binding site. As a result, the P_9 position becomes important in defining the bound structure. Further evidence for this turn structure is also seen in 2D NMR spectra of the bound peptide (*11*−*13*).

The thrombin receptor segment PAR1 (29−45) has a binding mode distinct from Fbg Aα (7−16) in which only the P_4−P_1 residues interact with the enzyme surface. Furthermore, PAR1 has the more optimal Pro at the P_2 position. The X-ray crystal structure of a thrombin-bound PAR1 segment ^{38}LDPR^{41} shows this Pro interacting effectively with the apolar binding site (*14*). The Leu at P_4 provides another important contact with this thrombin site. The high K_m value reported for PAR1 (29−45) reflects a reduced ability of this short peptide to accommodate the acidic Asp in the P_3 position (*2*).

Factor XIII has a more suitable P_4−P_1 segment, ^{34}VVPR^{37}, compared to the thrombin receptor PAR1. Val^{35} replaces the Asp and Val^{34} replaces the Leu, providing two residues for possible binding in the apolar binding site. The FXIII AP segment (28−41) has been shown to be a better substrate, with a K_m value approximately half that of PAR1 (29−45) (*15*). FXIII AP (28−41) contains Gly^{33} in a pivot position analogous to Gly^{12} in fibrinopeptide A; however, Val^{29} in FXIII AP occurs in place of the Phe^8 of fibrinopeptide A. The K_m of Fbg Aα (7−20) is about one-half that of FXIII AP (28−41), implying that the Phe^8-to-aryl binding pocket interaction more than compensates for the absence of a Pro in the P_2 site (*15*, *16*). FXIII AP (28−41) has features of the thrombin receptor and features of Fbg Aα (7−20), and its kinetics reflect binding characteristics in between.

Nature has provided a FXIII with a Val^{34} to Leu substitution. A Leu at position 34 in the activation peptide is a common human FXIII polymorphism, existing in approximately 20% of the European caucasian, 40% of the native American Pima, and 13% of the South Asian populations (*17*−*20*). FXIII V34L has been correlated in numerous studies with protection from myocardial infarction (*21*−*23*), ischaemic stroke (*24*), and venous thrombosis (*25*, *26*). Surprisingly, as a substrate for thrombin, FXIII V34L represents an improvement over FXIII V34, as indicated by an increase in k_{cat}/K_m (*15*, *20*, *27*). Furthermore, FXIII V34L has an increased rate of incorporation of α_2-antiplasmin into the clot structure, thus increasing resistance to thrombolysis (*28*). Electron micrograph studies, by Ariëns et al. (*27*), of fibrin cross-linked by FXIII V34 versus FXIII V34L show a significant difference in clot morphology. A full explanation for the protective effects of factor XIII V34L remains elusive.

An X-ray crystal structure of FXIII AP (28−37) complexed with thrombin was recently published by Sadasivan et al. (*29*). Structures were presented for two different complexes found in the asymmetric unit. Both complexes exhibited a β-turn for FXIII AP (28−37), one more ordered than the other, with a conformation similar to that of Fbg Aα (7−16). Preliminary modeling results and an examination of newly generated X-ray crystals suggested that the Leu34 substitution could not be tolerated and would likely force the β-turn structure into a different conformation.

Kinetic and X-ray crystal results imply that interactions between FXIII AP and thrombin can readily be manipulated by a single amino acid substitution. Such information may be used in the design of factor XIII molecules that can be more or less easily activated. As a result, factor XIII molecules could be produced that function under specific physiological environments or for particular needs. More information, however, is needed on the extent to which the complete sequence (aa 28−37) must interact with the thrombin surface and the roles that individual amino acids play in such binding.

In this study, HPLC-based kinetic assays, 1D proton line broadening NMR, and 2D transferred NOESY techniques were employed to investigate in solution the structural features that govern the binding and hydrolysis of site-specific mutants of factor XIII AP. Kinetic results for hydrolysis of Fbg Aα (7−20), FXIII AP (28−41), and FXIII AP (28−41) V34L by thrombin were presented earlier (*15*). Kinetic studies have now been extended to examine the specifically designed peptides, FXIII AP (28−41) V29F and FXIII AP (28−41) V29F V34L. Hydrolysis of these different peptides indicates that the P_4 residue plays a larger role in binding and hydrolysis than the P_9 residue. For the first time, NMR studies have been carried out on wild-type and mutant FXIII AP segments both free in solution and bound to thrombin. The structural information obtained was compared with published structural results for bound Fbg Aα (7−16), FXIII AP (28−37), and PAR1 (30−41). NMR evidence supports a binding mode for the factor XIII APs that is more like the thrombin receptor PAR1 peptide than fibrinopeptide A. The key anchor points onto the thrombin surface are proposed to be located within the P_4−P_1 positions of the factor XIII AP segments.

EXPERIMENTAL PROCEDURES

Synthetic Peptides. The peptide based upon residues 7−20 of the human fibrinogen Aα chain was synthesized by solid-phase methodologies by the Cornell University Biotechnology Resource Center (Ithaca, NY). Peptides based upon residues 28−41 of the human factor XIII activation peptide sequence were synthesized by the Cornell University Biotechnology Resource Center, Genemed Synthesis (South San Francisco, CA), and Peptides International (Louisville, KY). The amino acid sequences of the peptides are as follows: Fbg Aα (7−20), Ac-DFLAEGGGVRGPRV-amide; FXIII AP (28−41), Ac-TVELQGVVPRGVNL-amide; FXIII AP (28−41) V34L, Ac-TVELQGLVPRGVNL-amide; FXIII AP (28−41) V29F, Ac-TFELQGVVPRGVNL-amide; FXIII AP (28−41) V29F V34L, Ac-TFELQGLVPRGVNL-amide. The

purity of the peptides was evaluated by analytical reversed-phase HPLC and/or capillary electrophoresis. Matrix-assisted laser desorption ionization time of flight (MALDI-TOF) measurements on an Applied Biosystems Voyager DE-Pro mass spectrometer were used to verify the peptide *m*/*z* values. The concentration of peptides in solution was determined by quantitative amino acid analysis (Cornell Biotechnology Resource Center).

Thrombin Preparation. Bovine thrombin was isolated and purified from bovine plasma barium citrate as described previously by Trumbo and Maurer (*15*) and Ni et al. (*30*). *Echis carinatus* snake venom was used to activate the thrombin, followed by purification with gel filtration and ion-exchange chromatography. The final concentration of protein was determined by using an extinction coefficient, $E^{1\%} = 19.5$ at 280 nm (*31*).

For this project, bovine thrombin was used as the enzyme, and the synthetic substrate peptides were based on human sequences. Thrombin exhibits a high conservation of sequence between human and bovine forms (*32*). There are no differences in the residues involving the active site, the thrombin β-insertion loop (also called the Trp^{60D} loop), or the allosteric Na^+ binding site. The minor differences that exist between species are not anticipated to interfere with interaction of the substrate peptides at the thrombin active site surface (*33*).

Kinetics. The HPLC-based kinetic assay methods were described previously (*15*). Briefly, hydrolysis was initiated by addition of bovine thrombin to a particular peptide solution. At regular intervals, an aliquot of this reaction mixture was removed, quenched in 12.5% H_3PO_4, and then analyzed by RP-HPLC. The hydrolysis product peak was integrated and the peak area converted to a concentration through a calibration equation. The final thrombin concentrations for the new peptides examined include 4.5 nM thrombin for FXIII AP (28−41) V29F and 2.2 nM for FXIII AP (28−41) V29F V34L. The peptide concentrations were 56.1−673.2 μM for FXIII AP (28−41) V29F and 146.7−607.8 μM for FXIII AP (28−41) V29F V34L.

Initial velocities (in micromolar per second) for the thrombin-catalyzed reactions were determined for each peptide concentration from the slopes of product concentration versus time plots. At least three independent trials were performed at each concentration. The resultant kinetic data were fit to the equation $V = V_{max}/(1 + K_m/[S])$ by nonlinear regression methods using the Marquardt−Levenberg algorithm in Sigma Plot (Jandel Scientific). K_m, V_{max}, and k_{cat} were calculated from the coefficients of this equation.

To ensure that lower pH conditions required for the planned NMR experiments did not disrupt enzyme−substrate interactions, the kinetics were repeated at pH 6 for thrombin hydrolysis of FXIII AP (28−41) and FXIII AP (28−41) V34L. As expected, hydrolysis rates did decrease at pH 6, but the relative differences between the kinetic parameters of the wild type and the mutant remained proportional to those reported earlier (*15*) for hydrolysis at pH 7.4.

Peptide Hydrolysis for NMR Samples and Calibration Curves. Hydrolyzed peptide was needed to create a calibration curve in the kinetic studies. Hydrolyzed peptides were also used in the NMR studies to ensure that binding of a single species, the hydrolyzed product, was being observed. Fbg Aα (7−20), FXIII AP (28−41), FXIII AP (28−41) V29F, FXIII AP (28−41) V34L, and FXIII AP (28−41) V29F V34L were hydrolyzed at the scissile R−X bond by incubation with an excess of thrombin at 25 °C for 1 h. The hydrolyzed segments, Fbg Aα (7−16), FXIII AP (28−37), FXIII AP (28−37) V29F, FXIII AP (28−37) V34L, and FXIII AP (28−37) V29F V34L, were isolated and purified by reversed-phase HPLC (described previously in ref *15*). The fractions containing the ten-residue hydrolyzed peptides were verified by MALDI-TOF mass spectrometry and then lyophilized. The peptides were resolubilized in 400 μL of deionized water (dIH_2O) each and stored at 4 °C.

1D Proton Line Broadening and trNOESY Experiments. 1D proton line broadening and 2D transferred nuclear Overhauser effect (trNOESY) experiments (*34*−*36*) were used to investigate *in solution* the structural features that govern the activation of FXIII. When free in solution, peptides 10−15 amino acids in length tumble rapidly and, generally, have little secondary structure. $\omega\tau_c$ approaches 1, giving a sharp 1D spectrum and a transferred NOESY spectrum with few NOEs. When bound to the surface of an enzyme, the same peptide gains secondary structural features. A macromolecular complex with an increased $\omega\tau_c$ is created and promotes formation of large negative NOEs that describe the bound state of the peptide. In a complex, where the peptide concentration is in molar excess of the enzyme and k_{off} for the peptide is fast, information about this bound state is carried with the peptide as it rejoins the free population. The NOEs describing the bound conformation are much larger than any NOE for free peptide; thus, bound information dominates the NOESY spectrum. $\omega\tau_c$ is inversely proportional to the transverse relaxation time (T_2), and T_2 is related to the line width shape of the resonance. As $\omega\tau_c$ increases, T_2 decreases, thereby causing the line broadening effect in the 1D spectrum for any proton that comes in contact with the enzyme surface. If protons on the peptide enter a new chemical environment as they contact the surface of the enzyme, a change in chemical shift is possible and contributes to line broadening.

NMR Sample Preparation. NMR samples were prepared so that approximately a 1:10 enzyme-to-peptide ratio was maintained. For each peptide, 90 μL of NMR buffer (25 mM phosphate, 150 mM NaCl, 0.2 mM EDTA, pH 5.6) was added to the appropriate volume of hydrolyzed peptide solution. dIH_2O was added to bring the total volume of the peptide solution to 800 μL. Phosphates have diminished buffering capacity around the desired pH; therefore, the pH of the peptide stock solution was adjusted to 6 with NaOH to avoid precipitation problems with thrombin during sample preparation. Thrombin experiences a significant decrease in solubility below pH 5.3. The peptide solution was lyophilized and then resolubilized in 90 μL of D_2O to a concentration of 15 mM. Activated bovine thrombin in Mono S buffer (25 mM H_3PO_4, 280 mM NaCl, pH 6.5) was exchanged into NMR buffer by ultrafiltration (Beckman J2-HS centrifuge, JA-20 rotor, 5500 rpm, 4 °C) using a Centricon 10 ultrafiltration tube (Amicon) with a YM-10 membrane. The final volume of enzyme solution was adjusted to 360 μL with NMR buffer. Peptide/D_2O solution (40 μL) was added for a total sample volume of 400 μL. A free peptide sample, containing 360 μL of NMR buffer and 40 μL of peptide/D_2O solution, was made in parallel. The final concentration of enzyme in each enzyme−peptide sample was approxi-

mately 150 μM. The final concentration of peptide in each sample was approximately 1.50 mM. Peptide samples contained 10% v/v D_2O for a NMR signal lock. NMR experiments were carried out in susceptibility-matched 5 mm Shigemi NMR tubes (Shigemi, Tokyo, Japan).

NMR Analysis. The spectra were acquired at approximately 17 °C on a 500 MHz Varian Inova NMR spectrometer, equipped with a triple resonance probe and *z*-axis pulsed field gradients. Water was suppressed in one-dimensional and trNOESY experiments with the WET pulse sequence (*37*) and in the total correlation spectroscopy (TOCSY) experiments by presaturation. 1D spectra were acquired with 32 scans. Two-dimensional tnTOCSY experiments had 16 scans per FID, 512 t_1 increments, and a mixing time of 46 ms. 2D trNOESY experiments had 32 scans per FID, 512 t_1 increments, and a mixing time of 400 ms. The spectra were processed with Felix 2000 (MSI, San Diego, CA) on a Silicon Graphics 02 workstation. A 90° sine-bell apodization function was applied to both dimensions in each spectrum. Residual water signal was removed by convolution.

Chemical shift assignments for the protons of each peptide were derived from the TOCSY spectra. trNOESY spectra were then used to assign the sequential order for residues that appear more than once within the peptides. Proton chemical shifts were referenced with respect to the methyl protons of DSS at 0 ppm. Chemical shift assignments for all peptides may be seen in Tables 3−7 (Supporting Information).

RESULTS

Hydrolysis of Substrate-like Peptides by Thrombin. HPLC was used to monitor thrombin hydrolysis of fibrinogen Aα-like and FXIII AP-like peptides. Thrombin cleaved Fbg Aα (7−20) at the Arg^{16}−Gly^{17} peptide bond and cleaved the FXIII activation peptides at the Arg^{37}−Gly^{38} peptide bond. The hydrolyzed products eluted from a Brownlee Aquapore C8 column as distinct peaks from the parent substrate. The identities of these product peaks were verified by MALDI-TOF mass spectrometry. When the structural integrity of native fibrinogen is compromised, cleavage may occur at the Arg^{19}−Val^{20} peptide bond (reviewed in ref *38*). Cleavage at this secondary site has not been observed for the Fbg Aα (7−20) peptide under the solution conditions tested. No potential secondary cleavage site is present in FXIII AP (28−41).

Kinetic Evaluation of Thrombin Hydrolysis of Substrate-like Peptides. An HPLC-based assay was used in these kinetic studies. Nonlinear regression analysis values for K_m, k_{cat}, and k_{cat}/K_m are shown in Table 2. Results for Fbg Aα (7−20), FXIII AP (28−41), and FXIII AP (28−41) V34L were reported previously (*15*). Their kinetic parameters are included in the table so that direct comparisons can be made with the two new peptides examined, FXIII AP (28−41) V29F and FXIII AP (28−41) V29F V34L.

FXIII AP (28−41) V29F showed changes in kinetic parameters different from those observed for the wild-type and V34L activation peptide segments. Nonlinear regression analysis for thrombin hydrolysis of this peptide revealed a K_m of 195 ± 34 μM, a k_{cat} of 6.2 ± 0.43 s^{-1}, and a k_{cat}/K_m of 0.032 ± 0.006 μM^{-1} s^{-1}. FXIII AP (28−41) V29F has a K_m 1.6-fold lower and a k_{cat} 6.3-fold lower than with Fbg Aα (7−20). These new values compared to values for the wild-type FXIII segment showed a reduction in K_m by a factor of 2.6 but the same k_{cat} within experimental error.

Table 2: Kinetic Constants for the Hydrolysis of Arg−Xaa Bonds by Thrombin[a]

substrate peptide	K_m (μM)	k_{cat} (s^{-1})	k_{cat}/K_m ($\mu M^{-1} s^{-1}$)
Fbg Aα (7−20)[b]	312 ± 42	39.3 ± 2.6	0.126 ± 0.019
FXIII AP (28−41)[b]	508 ± 44	6.4 ± 0.03	0.013 ± 0.001
FXIII AP (28−41) V34L[b]	272 ± 57	18.5 ± 1.6	0.068 ± 0.015
FXIII AP (28−41) V29F	195 ± 34	6.2 ± 0.43	0.032 ± 0.006
FXIII AP (28−41) V29F V34L	352 ± 77	27.5 ± 2.9	0.078 ± 0.019
PAR1 (29−45)[c]	900	35	0.04

[a] Kinetic constants for thrombin-catalyzed hydrolysis of peptides based on the fibrinogen Aα chain and the factor XIII activation peptide segment were determined from an HPLC assay as described under Experimental Procedures. The results shown here represent averages for at least three independent experiments. Kinetic values reported were calculated using nonlinear regression analysis methods. [b] Results published previously (*15*). [c] Vu et al. (*2*).

FXIII AP (28−41) V29F V34L had a K_m comparable to Fbg Aα (7−20) and FXIII AP (28−41) V34L with a value of 352 ± 77 μM. This was 1.8-fold more than the K_m for FXIII AP (28−41) V29F and 1.4-fold less than the K_m for FXIII AP (28−41). The k_{cat} at 27.5 ± 2.9 s^{-1} was 4.4-fold greater than FXIII AP (28−41) V29F and 1.5-fold greater than for FXIII AP (28−41) V34L. This result leads to a k_{cat}/K_m slightly improved over FXIII AP (28−41) V34L, with a value of 0.078 ± 0.019 μM^{-1} s^{-1}.

One-Dimensional Line Broadening NMR for Wild-Type and Mutant FXIII AP-like Segments. One-dimensional proton NMR spectra were acquired for each hydrolyzed FXIII AP-like peptide segment free in solution and complexed with thrombin. Although the amide regions are shown for clarity, proton line broadening is seen through the full spectral range of the indicated residues, except as noted. A comparison of the spectra for the peptides with and without enzyme indicated that there were no significant changes in chemical shift upon binding to thrombin. The only changes observed occur upon thrombin hydrolysis of the Arg−Gly bonds in the different FXIII AP (28−41) segments and in Fbg Aα (7−20) to produce a new Arg C-terminus.

Figure 1 highlights the amide region of the 1D proton spectrum of FXIII AP (28−37). Spectrum A is the free peptide, and spectrum B is the peptide−enzyme complex. Line broadening for residues Gly^{33} through Arg^{37} is readily apparent. Neither Thr^{28}, Val^{29}, nor Glu^{30} showed broadening, indicating limited enzyme surface interactions over this portion of the peptide.

The spectra for FXIII AP (28−37) V34L are shown in Figure 2. Spectrum C highlights the amide region of the free peptide, and spectrum D shows the same region of the peptide−enzyme complex. Residues Leu^{34} through Arg^{37} constitute the majority of the broadened resonances. Broadening for the P_4 residue Leu^{34} is enhanced over Val^{34} of the wild-type peptide. As with FXIII AP (28−37), Thr^{28}, Val^{29}, and Glu^{30} were not broadened in the spectrum for the peptide−enzyme complex.

A dramatic increase in proton line broadening occurred in the spectrum for the FXIII AP (28−37) V29F−thrombin

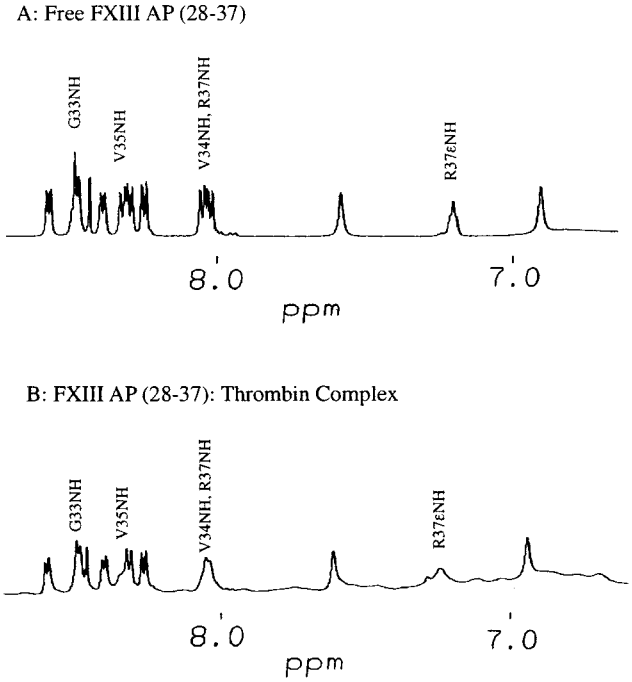

FIGURE 1: Line broadening in 1D proton NMR spectra for 1.5 mM factor XIII AP (28−37). (A) Spectrum for free peptide in solution. (B) Spectrum for peptide in the presence of 150 μM thrombin.

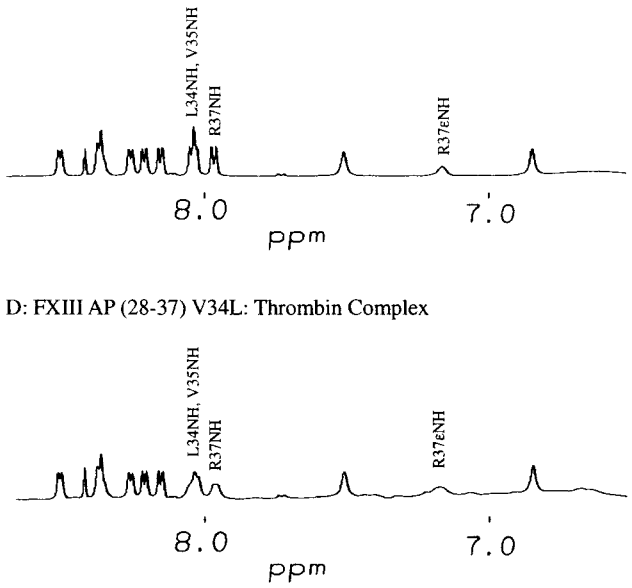

FIGURE 2: Line broadening in 1D proton NMR spectra for 1.5 mM factor XIII AP (28−37) V34L. (C) Spectrum for free peptide in solution. (D) Spectrum for peptide in the presence of 150 μM thrombin.

complex. Figure 3 shows the amide region of the 1D spectrum. Spectrum E is the free peptide, and spectrum F is the complex. Additional line broadening was observed for Phe[29], Glu[30], and Gln[32]. The Gly[33] through Arg[37] line broadening effects remained. FXIII AP (28−37) V29F is the first FXIII activation peptide-like substrate that presents clear NMR evidence for additional interactions of the N-terminus of the peptide with the thrombin surface.

When both mutations are present, in FXIII AP (28−37) V29F V34L, different residues were broadened than with either V29F or V34L alone. Some of the broadening with

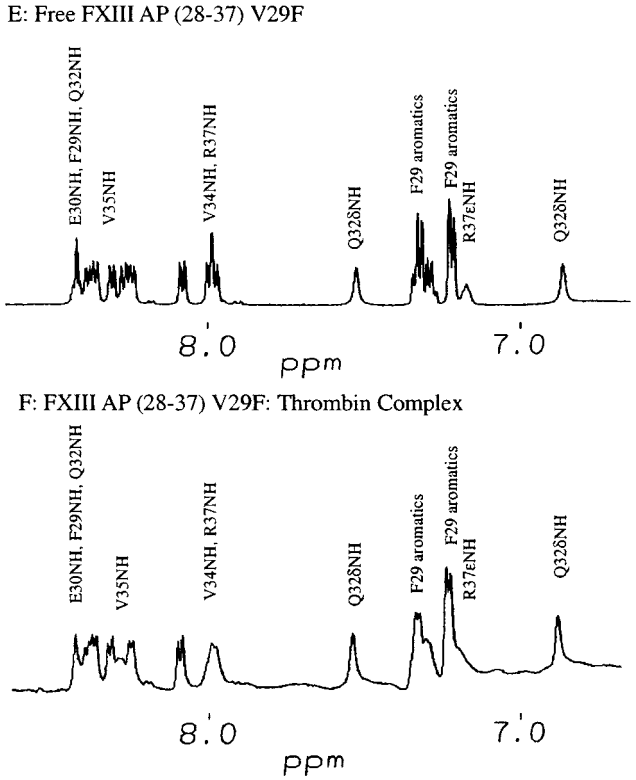

FIGURE 3: Line broadening in 1D proton NMR spectra for 1.5 mM factor XIII AP (28−37) V29F. (E) Spectrum for free peptide in solution. (F) Spectrum for peptide in the presence of 150 μM thrombin.

the V29F-only peptide disappeared, but there were new broadening effects not seen in the V34L-only peptide. The amide regions of the 1D spectra for FXIII AP (28−37) V29F V34L are in Figure 4. Spectrum G is the free peptide, and spectrum H is the peptide−enzyme complex. In the amide, aromatic, and amine proton regions, from 6.5 to 9 ppm, broadening was visible for Leu[31], Val[34], Val[35], and Arg[37], but any effect from Thr[28], Phe[29], and Glu[30] was lost. In the aliphatic region, from 0.5 to 4.5 ppm, broadening effects were retained for Phe[29]β' and Glu[30] protons and the remaining residues toward the C-terminus.

Two-Dimensional Transferred Nuclear Overhauser Effect NMR. Several pieces of evidence support a fast exchange process for the peptide−thrombin complexes. The K_m values are consistent with weak binding. For the NMR studies, proton line broadening is maintained at reduced temperatures, and large negative NOEs are present in the trNOESY spectra. Finally, there are no distorted peaks showing free and bound character, as seen in work on Fbg Aα (7−16) V15P, an improved thrombin substrate studied by Ni et al. (*12*).

Spectra of the peptide−thrombin complexes showed substantially more NOEs than spectra of free peptides (not shown) due to the peptide binding to the enzyme surface. Highlighted sections of the aliphatic−aliphatic proton regions of the different FXIII AP segments are shown in Figure 5. For all of the activation peptides, there was NOE evidence for side chain associations between V[35]γ and P[36]δ and δ'. In the spectra for the two L[34]-containing peptides, there was an additional interaction that was not visible in the V[34]-containing peptides, L[34]δ to P[36]δ. Through-space interactions from the V[34] side chain to the P[36] ring were not observed.

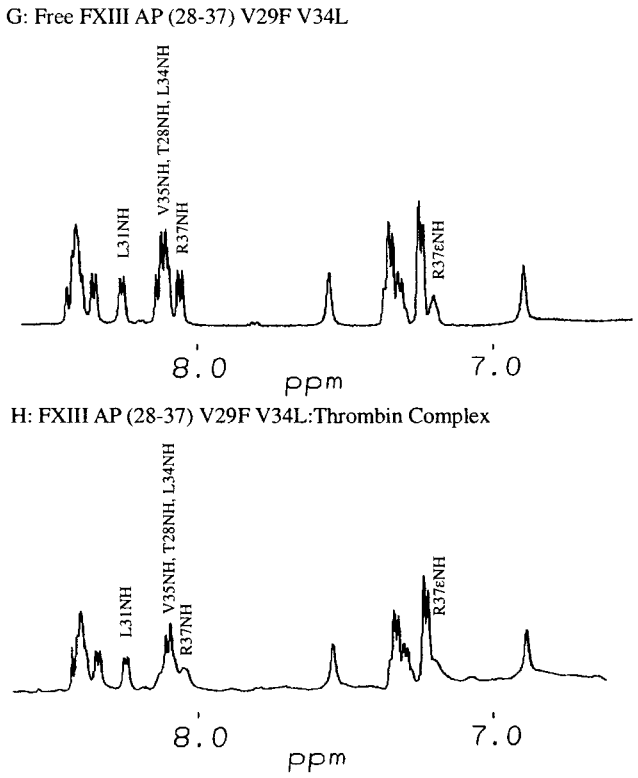

FIGURE 4: Line broadening in 1D proton NMR spectra for 1.5 mM factor XIII AP (28−37) V29F V34L. (G) Spectrum for free peptide in solution. (H) Spectrum for peptide in the presence of 150 μM thrombin.

NOEs for the aromatic−aliphatic side chain regions of FXIII AP (28−37), Fbg Aα (7−16), and FXIII AP (28−37) V29F are displayed in Figure 6. Evidence for the type I β-turn observed for Fbg Aα (7−16) is presented in the center panel, showing long-range NOEs involving Phe[8] (F[8]). There were clear NOEs between F[8]δ, ϵ, ζ and G[13/14]α, with ϵ being the strongest. Further NOEs were seen between F[8]δ, ϵ, ζ and V[15]α and γ. The hydrophobic cluster that results from the semi-α-helical portion of the bound peptide was evident in NOEs from the F8 aromatic side chain to the side chains of D7 and L9. These results agree with data published by Ni et al. (*11*, *12*, *30*), Maurer et al. (*39*), and Stubbs et al. (*13*). Corresponding NOEs from V[29] to V[35] or P[36], including V[29]γ−P[36]δ, are not present in spectra of the FXIII activation peptide segments. Despite the replacement of the Val at position 29 with a Phe, such long-range interactions were still not visible in the spectrum of FXIII AP (28−37) V29F.

FXIII AP (28−37) V29F V34L shows NOEs similar to those of FXIII AP (28−37) V29F. The only addition is an NOE from L[34]δ to P[36]δ, supporting the importance of the Leu[34] polymorphism of FXIII. Further NOEs exist between V[35]α and P[36]δ/δ' for all of the activation peptide segments. The F[29] activation peptides show an NOE from Phe[29]β/β' to Glu[30]NH versus no Val[29] side chain to E[30]NH interactions in the V29 activation peptides.

DISCUSSION

The peptide substrates analyzed contain amino acids that only interact with thrombin along a surface surrounding the enzyme active site. With peptides of this length, the influence of individual substrate amino acids on the binding and catalytic properties of thrombin can be examined. Emphasis is placed on the amino acids N-terminal to the R−X cleavage site.

NMR and Kinetic Studies Indicate the Importance of the P_4 Residue in the Activation of FXIII. A Val to Leu substitution at the P_4 position of the FXIII AP segment generates an enzyme that is more easily activated by thrombin. 1D proton line broadening NMR, 2D trNOESY, and kinetic studies suggest that the extra methylene group on Leu[34] provides an additional interaction point for the P_4 residue with the apolar binding site of thrombin. The [34]LVPR[37] segment makes critical contact with the thrombin surface, and new side chain−side chain NOE interactions involving Leu[34] and Pro[36] are observed that are not found for the V34 peptide. The further interaction at the P_4 site likely leads to the increased binding (lower K_m) to thrombin and also to the more efficient turnover rate of the Arg−Gly bond of FXIII AP (28−41) V34L (*15*). For both the wild-type and the V34L mutant sequence, no long-range NOE distances are observed from the N-terminal portion of the peptides toward the P_4−P_1 sequence. In addition, there are no proton line broadening effects for these N-terminal segments, further suggesting minimal if any contact with the thrombin enzyme surface.

The FXIII AP (28−41) V34L sequence has features in the P_4−P_1 sites that resemble those of the thrombin receptor PAR1 (29−45) segment. The X-ray crystal structure of a PAR1 (38−60)−thrombin complex published by Mathews et al. (*14*) confirmed the earlier published NMR structure of PAR1 (30−41) by Ni et al. (*40*). Both groups were able to show ordered structure for the P_4−P_1 residues followed by disordered segments for the residues outside this region. The Pro side chain in the P_2 position was tucked neatly into the apolar binding site. The side chain of Asp at P_3 extended away from the site to make a salt bridge with His[57] of thrombin's catalytic triad (*14*). The Leu[38] at P_4 had its side chain positioned near the Pro[40] at P_2, both within the thrombin apolar binding site. NMR evidence presented here supports a binding mode for FXIII AP (28−37) V34L much like that of PAR1 (30−41). Line broadening shows that surface interactions are focused between FXIII Leu[34] and Arg[37] which correspond to the P_4−P_1 positions.

The transferred NOESY spectra of PAR1 (30−41) by Ni et al. (*40*) and FXIII AP (28−37) V34L presented here both contain NOEs between the P_4 Leuδ protons and P_2 Proδ protons. NOEs also appear between FXIII AP (Val[35] α and Pro[36] δ/δ') and (Val[35] γ and Pro[36] δ/δ'). There are no through-space NOEs between the Val[35] side chain and either the Val[34] or Leu[34] side chain, suggesting that the Val[35] side chain is directed away from the apolar binding site. Overall, the peptide binds to the surface of thrombin in an extended conformation with an emphasis on the P_4−P_1 sites.

Additional NMR studies suggested that an extended conformation, similar to that of PAR1 and FXIII AP (28−37) V34L, also occurs for the bound wild-type FXIII AP (28−37). However, the X-ray crystal structure of wild-type FXIII (28−37) complexed to thrombin displays β-turn character involving the P_9−P_1 positions (*29*). Although not discussed by the authors, the bound structure for the P_4−P_1 peptide residues does have properties similar to that of PAR1. In the solution NMR studies presented here, the NOEs that would result from a β-turn structure have not been observed

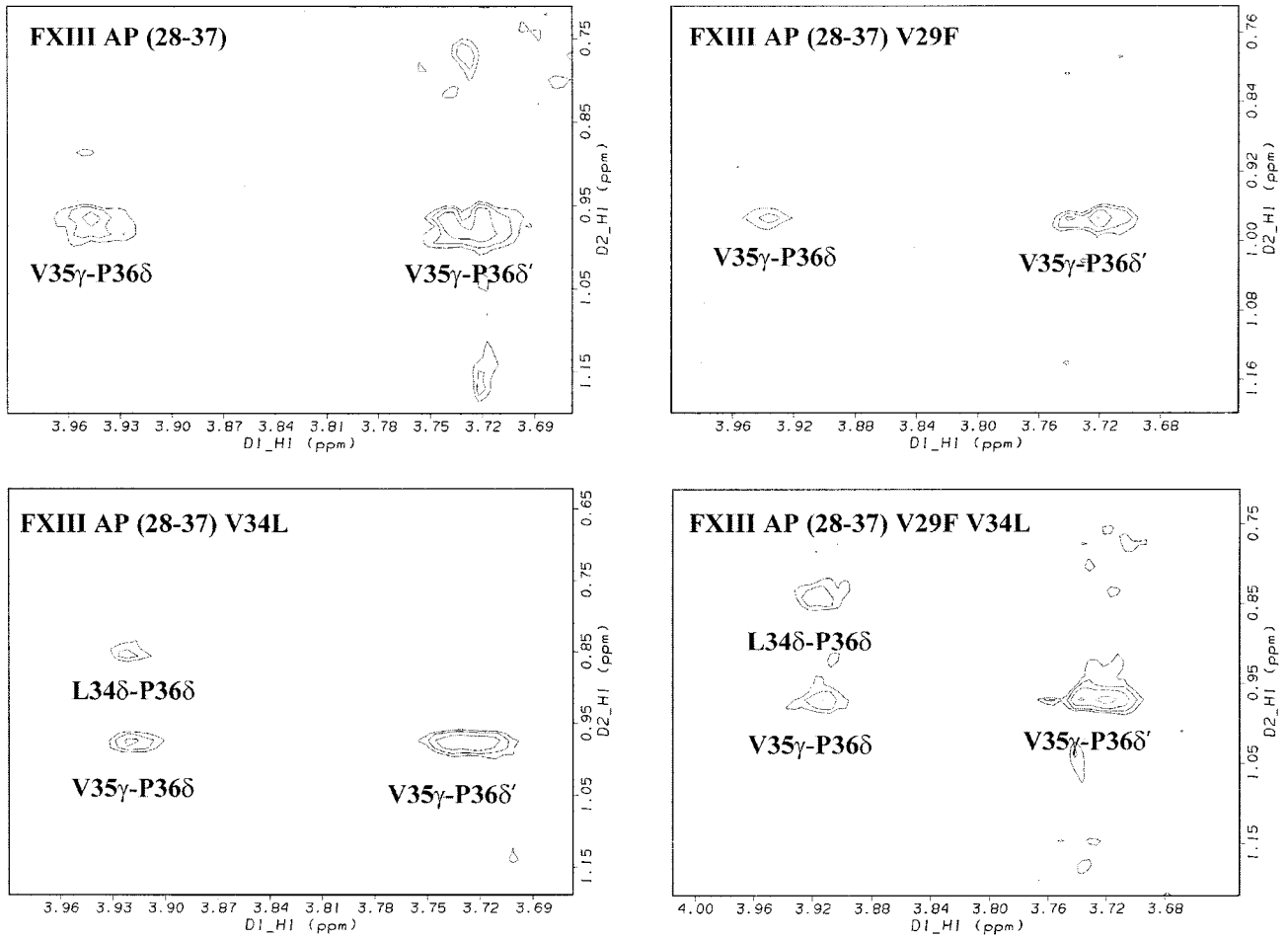

FIGURE 5: Comparison of aliphatic−aliphatic NOEs from 2D proton-transferred NOESY spectra for the activation peptide segments. Only the peptides with the V34L mutation have the position 34 side chain to Pro 36 δ NOE.

for the wild-type FXIII AP peptide. By contrast, a β-turn motif is clearly evident for Fbg Aα (7−16) bound to thrombin on the basis of both NMR and X-ray studies.

The interesting kinetics observed for the FXIII AP (28−41) V34L peptide versus the wild-type peptide suggest that FXIII activation can be controlled by single site substitutions. After comparison of the sequences of different thrombin substrates, FXIII (28−41) V29F was chosen for study. This sequence was based upon a desire to produce a hybrid between the FXIII AP and Fbg Aα (7−20). If the β-turn type moiety is a conserved feature of the wild-type FXIII AP segment, the V29F change may enhance this conformation and further mimic Fbg Aα (7−16). Indeed, the Val to Phe substitution in the P_9 position produced a substrate with improved binding over the wild type, as suggested by the decrease in K_m and the appearance of proton NMR line broadening for Phe[29], Glu[30], and Gln[32]. The Val[29]Phe substitution thus leads to better anchoring of the peptide on the enzyme surface. No change, however, occurred to k_{cat}, indicating that thrombin could hydrolyze the Arg−Gly bonds equally well in FXIII AP (28−41) V29F as in the wild type.

The trNOESY spectra of the bound FXIII AP (28−37) V29F were then examined for the presence of long-range distances involving Phe[29] that would support formation of a tighter β-turn. The only NOEs observed were sequential in nature, suggesting a predominantly extended conformation for the bound FXIII AP (28−37) (Figures 5 and 6). Phe[29] does contribute to surface binding, but if a β-turn does exist, the distances from the Phe toward the cleavage site must be too far to give NOEs (>5 Å). The hydrophobic surface on thrombin that is N-terminal to both the catalytic site and the Trp 60D insertion loop can likely accommodate a conformation other than the tight β-turn.

The doubly substituted activation peptide FXIII AP (28−41) V29F V34L shows that position 29 can serve as an anchor point for the activation peptide substrates, but position 34 plays a more influential role in binding and in the ability of thrombin to effectively hydrolyze the Arg[37]−Gly[38] bond. The K_m value indicates a binding affinity similar to the V34L-only substrate. Interestingly, there is a 4-fold improvement in k_{cat} over the wild type, consistent with thrombin hydrolyzing the Arg[37]−Gly[38] bond almost as easily as it does the Arg[16]−Gly[17] bond of Fbg Aα (7−20). Like the V34L-only substitution, the NMR spectrum shows the additional Leu[34]δ and the Pro[36]δ NOE, implying a closer through-space distance between these two amino acid positions in the apolar binding site compared to the wild type. A notable change occurs in the surface interaction of Phe[29] from the V29F V34L versus the V29F-only substrate. Line broadening shows that the aromatic and the β protons do not interact as well with the enzyme in comparison with the V29F-only substrate. This effect is further supported by an increase in K_m when compared with the V29F monosubstituted substrate. Apparently, as Leu[34] is more intimately associated with the apolar binding site, the binding enhancement offered by Phe[29] loses its importance.

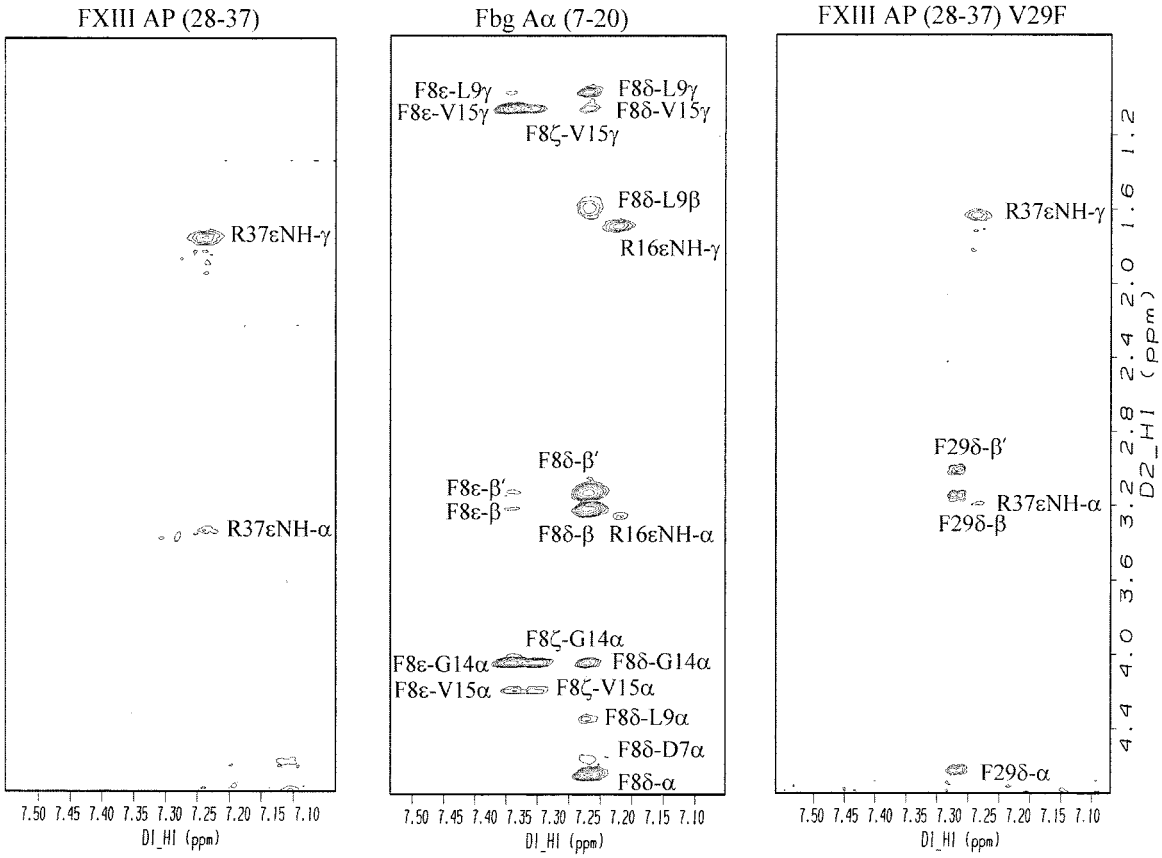

FIGURE 6: Comparison of aromatic−aliphatic NOEs from 2D proton-transferred NOESY spectra for FXIII AP (28−37), Fbg Aα (7−20), and FXIII AP (28−37) V29F. The spectrum for Fbg Aα (7−20) shows NOEs that indicate formation of a hydrophobic cluster between Phe[8], Leu[9], Gly[13/14], and Val[15]. Equivalent NOEs are not seen in the FXIII AP (28−37) V29F spectrum. The FXIII AP (28−37) spectrum is shown for comparison.

Evaluating NMR and X-ray Crystallographic Evidence Leads to a Hypothesis for the Binding Mode of FXIII AP (28−41) to Thrombin. Sadasivan et al. recently published X-ray crystal structures of FXIII AP (28−37) complexed with thrombin (*29*). Structures were proposed for two different complexes that formed in the crystal. PEP1 showed a well-ordered β-turn very similar to Fbg Aα (7−16) with interproton distances from the Val[29] side chain to Val[35] and Pro[36] within the range that should give NOEs in the trNOESY spectrum. PEP2 showed a less ordered β-turn, with interproton distances from the Val[29] side chain to Val[35] and Pro[36] unlikely to give rise to NOEs.

The NMR spectrum of the FXIII AP (28−37) segment complexed with thrombin showed no evidence of nonsequential interactions between Val[29] and any other amino acid in the peptide segment. This suggests that, if a β-turn conformation exists, either the protons of the residues involved are too distant from one another to give rise to NOEs or that the tighter formation is fleeting in nature. Under these conditions, a flexible β-turn motif is possible, with longer interproton distances from the Val[29] side chain to Val[35] and Pro[36], like PEP2 of the FXIII AP (28−37) X-ray crystal structure (*29*). The PEP2-containing complex does have higher *B*-factors than the PEP1-containing complex, possibly reflecting a greater degree of disorder for PEP2. The tighter β-turn observed for PEP1 bound to thrombin (MOL1) is held in place both by intramolecular contacts within this enzyme−peptide complex and also by intermolecular contacts with the MOL2 thrombin. By contrast, the PEP2 is not stabilized by intermolecular crystal contacts.

In the Sadasivan and Yee paper (*29*), the authors also make predictions about how the V34L mutant will interact with thrombin. From modeling studies and a review of newly generated crystals of FXIII (28−37) V34L, the authors suggest that the Leu substitution cannot be tolerated and would lead to a bound peptide conformation different from that of the β-turn. A structure similar to that observed in solution by NMR methods would accommodate this proposal. Upon the Val to Leu substitution, the N-terminal portion would be kicked out and the P_4-P_1 residues remain as the key anchor points. Kinetic and NMR results presented here suggest that such a conformation already has the tendency to form in solution with the wild-type Val.

The kinetic and NMR results collected on the FXIII AP peptides suggest that the N-terminal amino acids may be more free to accommodate different conformations than those of Fbg Aα (7−20). By contrast, a unique tight β-turn must be in place to compensate for the nonideal P_4-P_1 sequence of the Fbg Aα. Kinetic studies have demonstrated that including F[8] in the Fbg Aα-like peptide leads to an impressive 80-fold improvement in k_{cat}/K_m (*41*). The subtle fibrinogen Aα mutant F8Y, with a substitution in the P_9 position, cannot be accommodated within the active site surface as reported by both kinetic and X-ray studies (*42*, *43*). By contrast, the more significant FXIII V29F substitution is well tolerated by thrombin. If the β-turn were as important a structural feature in FXIII AP as in fibrinogen Aα, it seems likely that the FXIII AP would be locked in a conformation that could be observed by NMR and the P_9 position would exhibit a greater influence on structure and kinetics.

With this project, emphasis has been placed on comparing the P_9-P_1 positions of FXIII AP (28−37) with those of Fbg Aα (7−16) and PAR1 (29−45). Both kinetic and structural data are available for these different thrombin substrates. There are other fibrinogen-based sequences that are interesting to consider. With some non-native fibrinogen Aα sequences, cleavage may occur at the $R^{19}-V^{20}$ bond (*38*) with the P_4-P_1 residues being ^{16}RGPR^{19}. A Pro exists in the P_2 position, but there is a nonoptimal basic residue in the important P_4 position. Such an amino acid is likely to be difficult to accommodate. No structures are available on the binding of this RGPR sequence to thrombin. Upon removal of native fibrinogen Aα (1−16), a new N-terminus appears, starting with ^{17}GPRV^{20} that could be further cleaved by thrombin at $R^{19}-V^{20}$. This segment, however, is missing the important P_4 residue, and consistent with the P_4-P_1 model, cleavage is 5-fold slower at this site than at $R^{16}-G^{17}$ (*44*). In addition to interacting with fibrinogen Aα, thrombin also hydrolyzes the fibrinogen Bβ chain with the sequence ^{6}NEEGFFSAR^{14} occupying the P_9-P_1 positions. A Pro is not present at the P_2 position, but there is an intriguing Phe occupying the P_4 position. Future kinetic and structural studies on this Bβ sequence would aid in further defining the substrate specificity of thrombin.

Conclusions. The results collected support a binding mode in solution for FXIII AP (28−37) to thrombin resembling that displayed by the PAR1 segment, an extended conformation for the P_4-P_1 residues and a flexible N-terminus. Even with selective amino acid substitution, the extended conformation remains with additional peptide-to-enzyme contact provided by a larger side chain in V29F and/or V34L. The region most important for substrate specificity is P_4-P_1.

Evidence presented here firmly supports the ability to alter the activation of factor XIII through a single residue substitution. Substitution at the P_4 residue has an effect on both the K_m and k_{cat}. Such results suggest that this position affects not only binding but also the ability of thrombin to effectively hydrolyze the scissile bond. In contrast, substitution at the P_9 residue alters K_m only. By altering the amino acid at either the P_4 or P_9 position, one should be able to influence the rate and nature of factor XIII activation and, thus, the stability and resistance to thrombolysis of the covalently cross-linked fibrin clot.

ACKNOWLEDGMENT

We thank Dr. A. F. Spatola for generously providing access to the lyophilizer and Dr. N. J. Stolowich for assistance with the NMR instrumentation. We appreciate helpful discussions throughout the course of this research from D. Cleary, A. Marinescu, and B. Turner.

SUPPORTING INFORMATION AVAILABLE

Three tables listing the proton chemical shifts for the peptide segments studied. This material is available free of charge via the Internet at http://pubs.acs.org.

REFERENCES

1. Halkier, T. (1991) in *Mechanisms in Blood Coagulation Fibrinolysis and the Complement System*, pp 3−103, Cambridge University Press, Cambridge.
2. Vu, T.-K. H., Wheaton, V. I., Hung, D. T., Charo, I., and Coughlin, S. R. (1991) *Nature 353*, 674−677.
3. Esmon, N. L., Owen, W. G., and Esmon, C. T. (1982) *J. Biol. Chem. 257*, 859−864.
4. Stubbs, M. T., and Bode, W. (1993) *Thromb. Res. 69*, 1−58.
5. Vindigni, A., Dang, Q. D., and Di Cera, E. (1997) *Nat. Biotechol. 15*, 891−894.
6. Le Bonniec, B. F., Myles, T., Johnson, T., Knight, C. G., Tapparelli, C., and Stone, S. R. (1996) *Biochemistry 35*, 7114−7122.
7. Schechter, I., and Berger, A. (1968) *Biochem. Biophys. Res. Commun. 32*, 898−902.
8. Ichinose, A., and Davie, E. W. (1988) *Proc. Natl. Acad. Sci. U.S.A. 85*, 5829−5833.
9. Watt, K. W., Cottrell, B. A., Strong, D. O., and Doolittle, R. F. (1979) *Biochemistry 18*, 5410−5416.
10. Martin, P. D., Robertson, W., Turk, D., Huber, R., Bode, W., and Edwards, B. F. P. (1992) *J. Biol. Chem. 267*, 7911−7920.
11. Ni, F., Meinwald, Y. C., Vásquez, M., and Scheraga, H. A. (1989) *Biochemistry 28*, 3094−3105.
12. Ni, F., Zhu, Y., and Scheraga, H. A. (1995) *J. Mol. Biol. 252*, 656−671.
13. Stubbs, S. T., Oschkinat, H., Mayr, I., Huber, R., Angliker, H. A., Stone, S. R., and Bode, W. (1992) *Eur. J. Biochem. 206*, 189−195.
14. Mathews, I. I., Padmanabhan, K. P., Ganesh, V., Tulinsky, A., Ishii, M., Chen, J., Turck, C. W., Coughlin, S. R., and Fenton, J. W. (1994) *Biochemistry 33*, 3266−3279.
15. Trumbo, T. A., and Maurer, M. C. (2000) *J. Biol. Chem. 27*, 20627−20631.
16. Scheraga, H. A. (1983) *Ann. N.Y. Acad. Sci. 408*, 330−343.
17. Kohler, H. P., and Grant, P. J. (1999) *Q. J. Med. 92*, 67−72.
18. McCormack, L. J., Kain, K., Catto, A. J., Kohler, H. P., Stickland, M. H., and Grant, P. J. (1998) *Thromb. Haemostasis 80*, 523−524.
19. Anwar, R., and Miloszewski, K. J. A. (1999) *Br. J. Haematol. 107*, 468−484.
20. Kangsadalampai, S., and Board, P. G. (1998) *Blood 92*, 2766−2770.
21. Kohler, H. P., Futers, T. S., and Grant, P. J. (1999) *Thromb. Haemostasis 81*, 511−515.
22. Kohler, H. P., Stickland, M. H., Ossei-Gerning, N., Carter, A., Mikkola, H., and Grant, P. J. (1998) *Thromb. Haemostasis 79*, 8−13.
23. Wartiovaara, U., Perola, M., Mikkola, H., Tötterman, K., Savolainen, V., Penntilä, A., Grant, P. J., Tikkanen, M. J., Vartiainen, E., Karhunen, P. J., Peltonen, L., and Palotie, A. (1999) *Athersclerosis 142*, 295−300.
24. Catto, A. J., Kohler, H. P., Bannan, S., Stickland, M., Carter, A., and Grant, P. J. (1998) *Stroke 29*, 813−816.
25. Franco, R. F., Reitsma, P. H., Lourenco, D., Maffei, F. H., Morelli, V., Tavella, M. H., Araujo, A. G., Piccinato, C. E., and Zago, M. A. (1999) *Thromb. Haemostasis 81*, 676−679.
26. Catto, A. J., Kohler, H. P., Coore, J., Mansfield, M. W., Stickland, M. H., and Grant, P. J. (1999) *Blood 93*, 906−908.
27. Ariëns, R. A. S., Philippou, H., Nagaswami, C., Weisel, J. W., Lane, D. A., and Grant, P. J. (2000) *Blood 96*, 988−995.
28. Schröder, V., and Kohler, H. P. (2000) *Thromb. Haemostasis 84*, 1128−1130.
29. Sadasivan, C., and Yee, V. C. (2000) *J. Biol. Chem. 275*, 36942−36948.
30. Ni, F., Konishi, Y., Frazier, R., Scheraga, H. A., and Lord, S. T. (1989) *Biochemistry 28*, 3082−3094.
31. Winzor, D. J., and Scheraga, H. A. (1964) *Arch. Biochem. Biophys. 104*, 202−207.
32. Bode, W., Turk, D., and Karshikov, A. (1992) *Protein Sci. 1*, 426−479.
33. Dang, Q. D., Sabetta, M., and Di Cera, E. (1997) *J. Biol. Chem. 272*, 19649−19651.
34. Ni, F., and Scheraga, H. A. (1994) *Acc. Chem. Res. 27*, 257−264.
35. Ni, F. (1994) *Prog. NMR Spectrosc. 26*, 517−606.
36. Campbell, A. P., and Sykes, B. D. (1993) *Annu. Rev. Biophys. Biomol. Struct. 22*, 99−122.

37. Smallcombe, S. H., Patt, S. L., and Keifer, P. A. (1995) *J. Magn. Reson., Ser. A 117*, 295−303.
38. Beck, E. A., and Furlan, M. (1984) in *Current Problems in Clinical Biochemistry: Variants of Human Fibrinogen*, pp 273−321, Hans Huber Publishers, Berne, West Germany.
39. Maurer, M. C., Peng, J.-L, An, S. S., Trosset, J.-Y, Henschen-Edman, A., and Scheraga, H. A. (1998) *Biochemistry 37*, 5888−5902.
40. Ni, F., Ripoll, D. R., Martin, P. D., and Edwards, B. F. P. (1992) *Biochemistry 31*, 11551−11557.
41. Marsh, H. C., Meinwald, Y. C., Lee, S., and Scheraga, H. A. (1982) *Biochemistry 21*, 6167−6171.
42. Malkowski, M. G., Martin, P. D., Lord, S. T., and Edwards, B. F. P. (1997) *Biochem. J. 326*, 815−822.
43. Lord, S. T., Byrd, P. A., Hede, K. L., Wei, C., and Colby, T. J. (1990) *J. Biol. Chem. 265*, 838−843.
44. Blomback, B., Blomback, M., Henschen, A., Hessel, B., Iwanaga, S., and Woods, K. R. (1968) *Nature 218*, 130−134.

BI0157823